CIRP Annals - Manufacturing Technology 58 (2009) 335–338

Contents lists available at ScienceDirect

CIRP Annals - Manufacturing Technology

journal homepage: http://ees.elsevier.com/cirp/default.asp

# Dynamic stiffness enhancement of direct-driven machine tools using sliding mode control with disturbance recovery

Y. Altintas (1)*, C.E. Okwudire

*Manufacturing Automation Laboratory, University of British Columbia, Vancouver, Canada*

ARTICLE INFO

*Keywords:*
Control
Drive
Linear motor

ABSTRACT

This paper presents a disturbance adaptive discrete sliding mode controller for feed drives equipped with linear motors. The control law is expressed as a function of friction and cutting force disturbances which are estimated from the motor force and control states. The accurate prediction of disturbance forces is used to actively compensate low frequency machine tool structural modes which are within the bandwidth of the controller. The proposed control system is experimentally demonstrated on a high performance linear drive, which exhibited high bandwidth and significant increase in dynamic stiffness compared to classical cascaded control methods.



## 1. Introduction

Direct drives are increasingly used as an alternative to ballscrew drives in high-speed machine tools. Compared to ballscrew drives, they can achieve higher speeds/accelerations and longer strokes, with less friction, zero backlash and no ballscrew axial-torsional vibrations which reduce the high-speed path tracking accuracy of the controllers [1].

However, a major drawback of direct drives is the absence of the mechanical stiffness and gear reduction ratio that is present in ballscrew drives [2]. Unlike in ballscrew drives, the cutting forces are transmitted directly to the linear motor, which must be oversized to have enough dynamic stiffness against external disturbance forces. The oversizing of linear motors needs to be reduced by designing control algorithms which have high bandwidth and strong rejection of cutting force disturbances.

Control laws are continuously improved to achieve higher bandwidth, better disturbance rejection and compensation of structural modes. Altintas et al. [3] presented an Adaptive Sliding Mode Controller (ASMC) with friction compensation of ballscrew drives, which increased the bandwidth and helped to minimize friction disturbances. Later, Kamalzadeh and Erkorkmaz [4] included the compensation of axial vibrations and ballscrew lead errors into an expanded ASMC. Dumur et al. [5] used the classical controller with cascaded position, velocity and current loops. However, they replaced the proportional position controller with a Generalized Predictive Controller in order to improve robustness and compensate a bending mode of the machine. Van Brussel and co-workers [6] used a two axis linear motor controlled by the classical Cascaded Controller. They modeled the friction on the guides and predicted the remaining unmodeled friction using an observer based on the inverse model of the machine dynamics. They added a repetitive controller to the position control loop, which reduced the effect of periodic cutting forces significantly and led to higher dynamic stiffness on the linear drives.

This paper presents a sliding mode controller with a friction and cutting force disturbance recovery to simultaneously achieve high bandwidth, cutting force prediction, and active compensation of structural vibrations of the machine. The proposed controller structure is similar to classical cascade controllers used in direct drives (hence it is easy to implement) but with significantly increased dynamic stiffness and improved cutting force estimates. Henceforth the paper is organized as follows. The design of the proposed Disturbance Adaptive Discrete Sliding Mode Controller and the structure of the classical Cascaded Controller together with a comparison of their performance are given in Section 2. The proposed disturbance force recovery and its use in active compensation of structural vibrations are presented in Section 3. The experimental validation of the proposed algorithms on a linear drive system is presented in Section 4, and the paper is concluded in Section 5.

## 2. Controller design

The linear drive is modeled by its rigid mass ($m$) and viscous damping ($b$) as,

$$m\ddot{x} + b\dot{x} = F_m(t) + F_d(t) \tag{1}$$

where $x$, $\dot{x}$ and $\ddot{x}$ are the actual position, velocity and acceleration of the drive while $F_m$ and $F_d$ are the linear motor force and disturbance cutting forces, respectively. The position error ($e_x = x_r - x$) and velocity error of the drive ($e_\upsilon = \dot{x}_r - \dot{x}$) can be represented in discrete time intervals, $T$ by applying backward Euler approximation,

$$\left.\begin{aligned} e_x(k) &= e_x(k-1) + Te_\upsilon(k) \\ e_\upsilon(k) &= e_\upsilon(k-1) + \frac{T}{m}(\ddot{x}_r + b\dot{x}(k) - F_m(k) - F_d(k)) \end{aligned}\right\} \tag{2}$$

where $k$ is the sampling counter while $x_r$, $\dot{x}_r$ and $\ddot{x}_r$ are the reference position, velocity and acceleration, respectively.

* Corresponding author.

0007-8506/$ – see front matter © 2009 CIRP.
doi:10.1016/j.cirp.2009.03.045

### 2.1. Disturbance Adaptive Discrete-Time Sliding Mode Controller (DADSC)

The Disturbance Adaptive Discrete-Time Sliding Mode Controller proposed by Won and Hedrick [7] is extended here to direct feed drive control with structural vibration compensation. A first order sliding controller surface $s(k)$ is designed to minimize both position and velocity errors as [3,7],

$$s(k) = \lambda e_x(k) + e_\upsilon(k) \tag{3}$$

where $\lambda$ is a gain indicating the bandwidth of the controller. The control force can be obtained by minimizing a Lyapunov function using a similar method as presented previously in [3,4,7],

$$F_m(k) = m\ddot{x}_r(k) + mKs(k) - \hat{F}_d(k) + b\dot{x}(k) + m\lambda e_\upsilon(k) \tag{4}$$

where $K$ is a feedback gain and $\hat{F}_d$ is the estimated disturbance force given by:

$$\hat{F}_d(k) = -\left(\frac{g_1 z - g_2}{z-1}\right)s(k) \tag{5}$$

with tunable adaptation gains $g_1$ and $g_2$. Substituting Eqs. (2), (4) and (5) into Eq. (3) and simplifying the result yields the sliding surface dynamics of the closed-loop system as:

$$\begin{Bmatrix} s(k) \\ \hat{F}_d(k) \end{Bmatrix} = \frac{1}{Q + g_1 R} \times \left( \begin{bmatrix} 1 + g_2 R & R \\ g_2 Q - g_1 & Q \end{bmatrix} \begin{Bmatrix} s(k-1) \\ \hat{F}_d(k-1) \end{Bmatrix} + \begin{Bmatrix} -R \\ g_1 R \end{Bmatrix} F_d(k) \right) \tag{6}$$

where $Q = 1 + KT$; $R = m^{-1}T$. The term $g_2Q - g_1$ in Eq. (6) determines the coupling between the disturbance force estimation and the sliding surface, which is eliminated by selecting $g_2 = Q^{-1}g_1$. The elimination of the coupling makes the DADSC to have better disturbance estimation than the cascade controllers used in present CNC systems.

### 2.2. Cascaded Controller (CC)

The widely used CC consists of cascaded velocity and position loops as shown in Fig. 1. The velocity loop is closed using a proportional integral (PI) while the position loop is closed using a proportional (P) controller. Velocity and acceleration feed-forward loops are also included in order to improve the reference tracking accuracy. $K_\upsilon$, $K_p$ and $T_i$ are the gains of the CC shown in Fig. 1.

From the block diagram of Fig. 1, the closed-loop dynamics of the CC is found in a similar form as in the DADSC:

$$\begin{Bmatrix} s(k) \\ \hat{F}_d(k) \end{Bmatrix} = \frac{1}{Q' + g_1' R} \left( \begin{bmatrix} 1 & R \\ -g_1' & Q' \end{bmatrix} \begin{Bmatrix} s(k-1) \\ \hat{F}_d(k-1) \end{Bmatrix} + \begin{Bmatrix} -R \\ g_1' R \end{Bmatrix} F_d(k) + \begin{Bmatrix} K_\upsilon T \\ -g_1' K_\upsilon T \end{Bmatrix} e_\upsilon(k) \right) \tag{7}$$

where $Q' = 1 + m^{-1}K_pT$; $g_1' = T_i^{-1}K_pT$.

### 2.3. Comparison of DADSC and CCs

Comparing the CC (Eq. (7)) to the DADSC (Eq. (6)) reveals that the disturbance estimation ($\hat{F}_d(k)$) cannot be decoupled from the equivalent sliding surface ($s(k)$) in the CC because $g_2 = 0$ in Eq. (7).

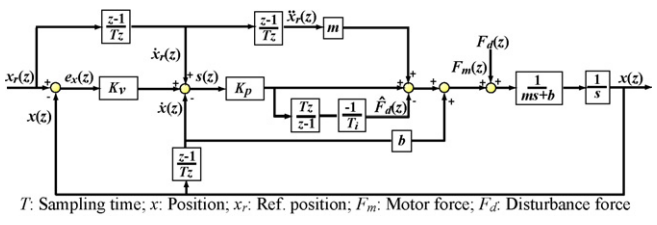


**Fig. 1.** Block diagram of a P–PI Cascaded Controller with velocity and acceleration feed-forward. $T$: sampling time; $x$: position; $x_r$: ref. position; $F_m$: motor force; $F_d$: disturbance force.

**Table 1**
Definition of coefficients of disturbance transfer function (Eq. (8)) for the DADSC and CC.

| Coefficient | $r_1$ | $r_2$ | $r_3$ | $r_4$ | $r_5$ |
|---|---|---|---|---|---|
| DADSC | $\lambda T + 1$ | $mK$ | $\lambda T + 1$ | $g_1$ | $Q^{-1}r_4$ |
| CC | 1 | $K_p$ | $K_\upsilon T + 1$ | $K_pT/T_i$ | 0 |

Furthermore, the velocity error term, $e_\upsilon(k)$ is not completely cancelled out of the closed-loop dynamics, hence it introduces errors in both the control function ($s(k)$) and estimated disturbance force ($\hat{F}_d(k)$). As a result, the DADSC has better disturbance rejection properties than the CC.

Let us assume that the drive is ideal and well represented by Eq. (1) for analytical comparison. The drive position tracking transfer function (TF), $x(z)/x_r(z)$, is unity for both controllers. The disturbance transfer function, $x(z)/F_d(z)$, is given for both controllers by the following:

$$\frac{x(z)}{F_d(z)} = \frac{T^2 z^2 (z-1)}{m(z-1)^2(r_1 z - 1) + r_2 T(z^2-1)(r_3 z - 1) + Tz(r_4 z - r_5)(r_3 z - 1)} \tag{8}$$

The coefficients $r_1$ to $r_5$ for the DADSC and CC are summarized in Table 1.

The advantage of the decoupled disturbance estimation and the cancelled velocity error term ($e_\upsilon$) in the DADSC is seen by increasing the feedback gain, $r_2$ and disturbance adaptation gain, $r_4$ steadily while keeping the other parameters constant. As shown in Fig. 2(a), as $r_2$ and $r_4$ are increased, the poles of the disturbance transfer function of the CC begin to leave the real axes, and the system becomes under-damped and oscillatory. However, no matter how much $r_2$ and $r_4$ are increased, the poles of the DADSC remain over-damped and never leave the real-axis. As we can see from the disturbance Bode plot (Fig. 2(b)) this results in an increased dynamic stiffness for the DADSC and makes it less susceptible to disturbances when compared to the Cascaded Controller.

## 3. Disturbance recovery and its application to active vibration control

Although the DADSC has better disturbance rejection than the CC, its estimated disturbance force, $\hat{F}_d(k)$ has a gain-dependent bandwidth which is often too low to be useful for practical purposes. Therefore, its disturbance estimation property is improved using a disturbance recovery (DR) algorithm presented here. The 'true' disturbance force $F_d(k)$ is extracted from Eq. (6) and expressed as a function of the estimated

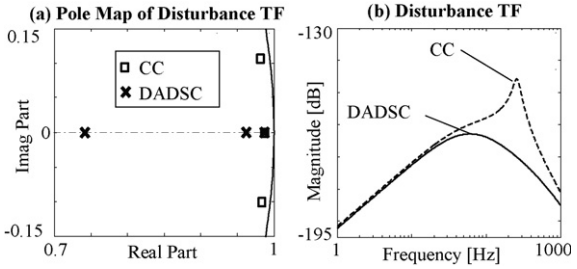


**Fig. 2.** Pole map and Bode magnitude plot of disturbance transfer function (TF) of the DADSC and CC. (a) Pole map of disturbance TF and (b) disturbance TF.